Pulsed laser deposited stoichiometric GaSb films for optoelectronic and phase change memory applications

Yimam, Daniel; Zhang, Heng; Momand, Jamo; Kooi, Bart

Published in:
Materials science in semiconductor processing

DOI:
10.1016/j.mssp.2021.105965

Publication date:
2021

Materials Science in Semiconductor Processing 133 (2021) 105965

Contents lists available at ScienceDirect

Materials Science in Semiconductor Processing

journal homepage: www.elsevier.com/locate/mssp

Pulsed laser deposited stoichiometric GaSb films for optoelectronic and phase change memory applications

Daniel T. Yimam *, Heng Zhang, Jamo Momand, Bart J. Kooi **

Zernike Institute for Advanced Materials, University of Groningen,Nijenborgh 4, 9747 AG Groningen, the Netherlands

ARTICLE INFO

Keywords:
Phase change materials
Pulsed laser deposition
GaSb thin Films
Target rotation

ABSTRACT

Phase-change memory (PCM) holds great potential in realizing the combination of DRAM-like speeds with non-volatility and large storage capacity for future electronic devices including in-memory computing. However, various (reliability) issues related to e.g. too high programming current (power consumption), resistance drift, data retention (low crystallization temperature), phase separation and density change upon switching stand in the way to make PCM really attractive. GaSb thin films have interesting optical and electrical properties which are attractive for optoelectronic and PCM applications but so far reported stoichiometric GaSb compositions are Sb-rich which produced reliability issues in PCM devices. In this study, we managed to deposit stoichiometric GaSb thin films using pulsed laser deposition (PLD) by varying deposition parameters and conditions. Using electron microscopy, the morphology of deposited films and target surface and the compositional deviation from exact stoichiometry have been investigated. We show that the directional nature of laser-target interaction is directly responsible for film quality in PLD in which particulates with high number density are generated due to directional pillar formation. Suppressing this pillar formation, by a simple 180° target rotation, showed an increase in deposition yield by 60%, exact stoichiometric transfer from target to substrate, and large reduction in particulate density. Moreover, from XRD analysis, we show that exact stoichiometric transfer from target to substrate is crucial for structural integrity of the produced films. Temperature induced structural transformation from resistivity vs. temperature measurements show a high crystallization temperature of 250 °C for stoichiometric GaSb thin film. We believe the exact stoichiometric GaSb thin films with reduced particulate densities and favorable structural and (opto)electronic properties are attractive for future PCM devices.

1. Introduction

Phase-Change Memory (PCM) architectures are some of the most promising candidates for future data storage devices [1]. In PCM, data is stored by using the large electrical resistivity or optical reflectivity contrast between the amorphous and crystalline phases. The switching between these phases is usually achieved by applying electrical or optical pulses, which by Joule heating either induce crystallization at elevated temperatures below the melting point or amorphization via melt-quenching, called SET and RESET operations, respectively [2–4]. By far the most studied materials for PCM applications are Ge-Sb-Te alloys [5,6]. In addition to the large resistivity contrasts, the fast reversible switching between amorphous and crystalline phases with nanoseconds crystallization speeds are the main attractive features for these materials [7]. However, many reliability issues hinder the full potential of PCM memory elements. For instance, the resistivity of the amorphous phase after the RESET pulse increases in time and this is commonly referred to as resistance drift [8,9]. This drift towards higher resistivity is caused by structural relaxation to a more favorable state with lower energy [10]. Also, during the SET-RESET operations volume changes occur in general due to structural transformation between the phases. This continuous contraction/expansion is known to cause voids between contact electrodes and the PCM element, reducing the cyclability of the device [11,12]. Furthermore, Ge-Sb-Te alloys suffer from electromigration particularly during the times they are in the liquid state [13]. Finally, the most studied PCM $Ge_2Sb_2Te_5$ (GST225) has a crystallization temperature of $<160\ ^{\circ}C$, which is relatively low for embedded applications [14]. These problems thus necessitate novel approaches to tailor PCMs for a wide range of emerging applications.

A lot of progress has been made to solve current problems with

* Corresponding author. ,
** Corresponding author.
E-mail addresses: d.t.yimam@rug.nl (D.T. Yimam), b.j.kooi@rug.nl (B.J. Kooi).

https://doi.org/10.1016/j.mssp.2021.105965
Received 15 March 2021; Received in revised form 5 May 2021; Accepted 20 May 2021
Available online 4 June 2021

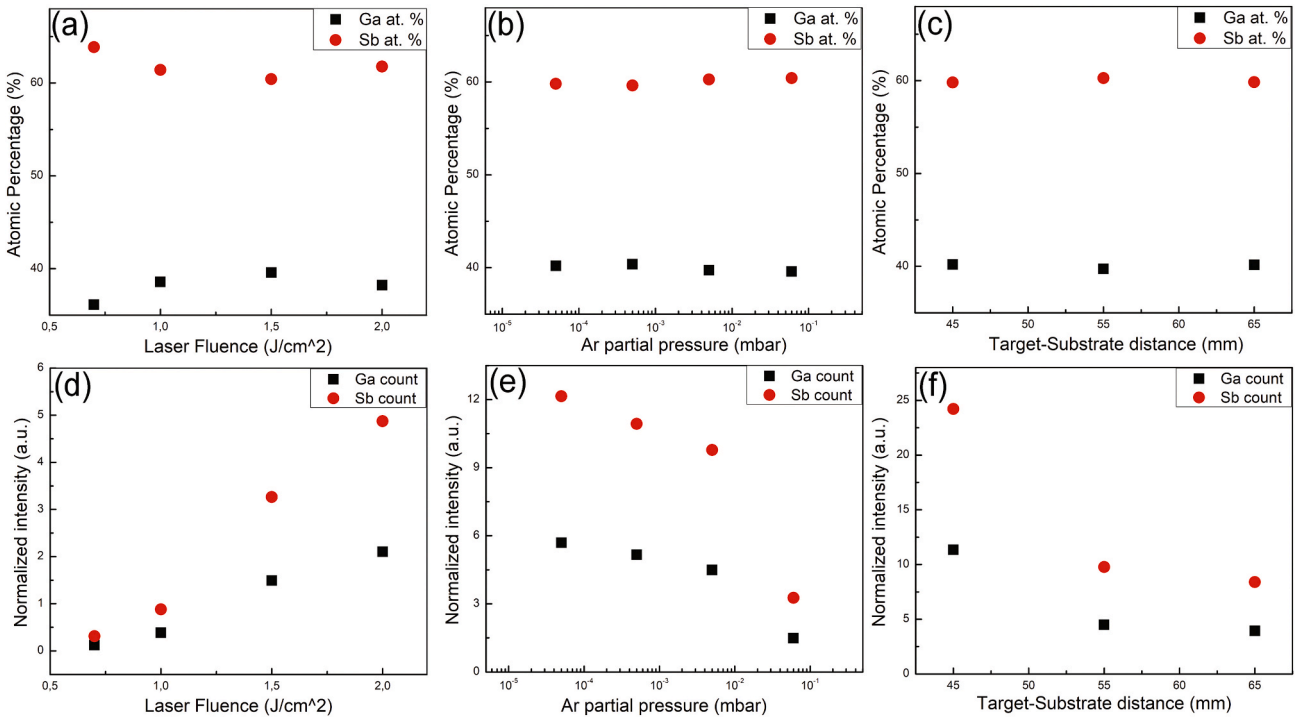

Fig. 1. TEM-EDX composition and yield analysis for a series of samples deposited using a powder sintered GaSb target by varying crucial PLD parameters. Ga and Sb composition analysis of deposited films by varying (a) laser fluence, (b) Ar process gas partial pressure, and (c) Target-Substrate distance. EDX intensity counts of Ga and Sb normalized with carbon intensity count in the spectrum as a function of (d) laser fluence, (e) Ar process gas partial pressure, and (f) Target-Substrate distance.

chalcogenide PCMs by composition tunning [14,15] and elemental doping [16]. Another approach is to go for a completely new phase change material with attractive properties altogether. Among those ideal for future PCM devices are GaSb alloys, which attract attention due to their unusual crystallization behavior [17]. For instance, GaSb exhibits a volumetric expansion instead of contraction upon crystallization, that leads to a negative optical contrast in the stoichiometric GaSb films [18]. In addition, varying Sb content in $Ga_{1-x}Sb_x$ is shown to affect the materials electrical and structural properties [19,20]. In fact, it has been shown that for a specific Sb content of $Ga_{30}Sb_{70}$ the density changes between phases disappear [21]. When used as a PCM device, the lack of density difference between phases would be advantageous to increase the device endurance and reduce resistance drift. However, a drawback of Sb-rich GaSb alloys is that they are highly susceptible to phase separation into Sb and (stoichiometric) GaSb. This problem is completely avoided when using stoichiometric GaSb as PCM. Moreover, GaSb is known to exhibit a much higher crystallization temperature (beyond 200 C) than the traditional PCM like GST225 (150 C). Stoichiometric GaSb is a stable phase without chemical driving force for phase separation. Although currently unclear, it can also be speculated that stoichiometric GaSb is more resistant to electromigration (in the liquid state). Therefore, more research on GaSb as a highly promising PCM is required.

Although not common for GaSb, Pulsed Laser Deposition (PLD) is a popular method of preparing chalcogenide thin films, both for optoelectronics and PCM applications [22–26]. PLD has become one of the common thin film deposition techniques in recent years. The processing speed, the flexibility, the scalability, applicability for wide range of materials, and cost effectiveness are among some of the reasons for its popularity [27]. One of the major drawbacks of PLD is the presence of micrometer sized particulates on the film surface [28]. This is a big problem for devices since the particulates not only alter material properties like optical reflectivity and electrical resistance, but also can destroy device architecture. Particulate production in PLD is considered inherent and it involves multiple parameters. The target used, the laser fluence, laser repetition rate, target substrate distance, and processing gas inside chamber all contribute to particulate generation. Researchers have given a lot of attention to lower the particulate density in PLD deposited thin films. Gas-jet injection into the chamber, directed towards the plasma plume, show reduction in particulate density [28,29]. Another example is the use of an additional laser to heat and vaporize the particulates in the plasma plume [30]. The micron size particulates are heavier than the constituents in the plasma plume and travel slower. Velocity filters in front of the plume were used to kick off particulates before reaching the substrate [31]. Although the yield is relatively low, another approach was to use an off-axis geometry to reduce particulate density where the substrate is shifted away from the plasma plume axis by a small distance [32]. Almost all works done involve reduction of particulates after their generation. Recently it has been shown that particulate generation can be suppressed by using a continuous target rotation to simulate irradiations in opposite directions [33]. However, none of these methods were effective in achieving ab-initio stoichiometric GaSb deposition that contains low particulate densities.

Thus, one of the major problems here is that PLD deposited GaSb suffers from high density of particulates on the film surface [34]. Thin films of GaSb are usually prepared by DC magnetron sputtering from GaSb targets [17,20]. Even though sputtered films are particulate free, the reported compositions are off-stoichiometric. In fact, for both PLD and magnetron sputtering, the reported elemental composition for stoichiometric GaSb is actually $Ga_{45}Sb_{55}$. However, when Sb content is increased in GaSb alloys their crystallization temperature seems to decrease and additional crystallization of the excess Sb will compromise the performance of PCM devices [17]. To incorporate GaSb into future PCM devices, problems with off-stoichiometric thin film production for both magnetron sputtering and PLD and high particulate densities on the film surface in PLD must be solved. In this work we show that particulate reduction/elimination and exact stoichiometric composition transfer can be achieved by PLD with the implementation of a 180° rotation holder. The film morphology and elemental composition have been studied by Scanning Electron Microscopy (SEM) and

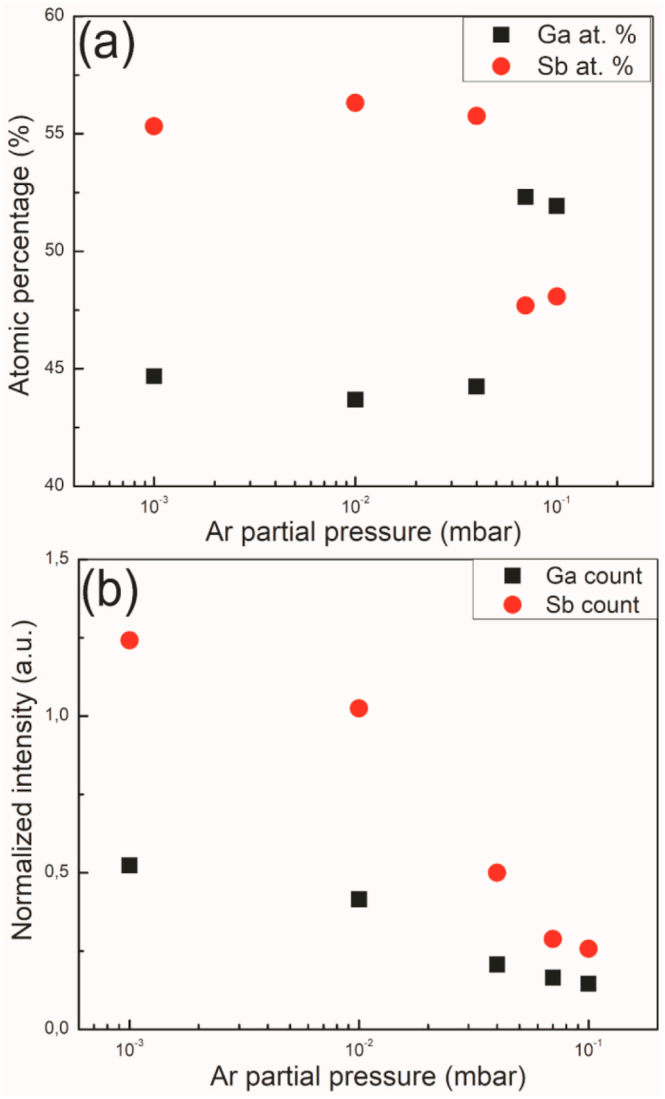

Fig. 2. TEM-EDX composition and yield analysis for a series of samples deposited using a homemade GaSb target. Laser fluence and Target-Substrate distances are fixed with values of 1.5 J cm^{-2} and 55 mm, respectively. (a) Ga and Sb composition analysis of deposited films for various Ar process gas partial pressures, and (b) EDX intensity counts of Ga and Sb normalized with carbon intensity count in the spectrum for various Ar process gas partial pressures.

Scanning/Transmission Electron Microscopy (S\TEM). To further investigate the properties of these particulate-free and stoichiometric films, structural analysis and electrical resistivity measurements have been performed by X-ray diffraction and Van der Pauw setup.

2. Experimental

2.1. Film deposition

We deposited GaSb thin films with pulsed laser deposition (PLD) on Si/SiO_2 substrates for X-ray diffraction (XRD) and electrical characterization and on continuous carbon and Si_3N_4 TEM grids for scanning transmission electron microscopy (S/TEM) analysis. Initially, we deposited GaSb with stoichiometric GaSb powder sintered targets from K-TECH. Later, we prepared stoichiometric GaSb targets by melting exact atomic portions of high-purity (5 N) Ga and Sb elements in a vacuum sealed quartz ampoule. The ampule was placed in an oven and left for 2 h at 750 °C before we took it out. Finally, for a PLD system using a KrF excimer laser (wavelength of 248 nm), we applied a fluence of 1.5 J cm^{-2}, processing gas (Ar) pressure of 10^{-3} mBar, while the substrate was kept at room temperature. The GaSb target was translated, normal to the substrate, through the scan area to induce continuous movement. During deposition, we either did not apply any target rotation or we rotated the target 180° after a certain number of laser pulses using a homemade target holder in addition to the translation (see Supplementary Information, Fig. S1).

2.2. Film characterization

The surface morphology and stoichiometry of targets and GaSb films were studied using scanning electron microscopy (SEM) (FEI NovaNanoSEM 650 and FEI Helios G4 CX), equipped with an energy dispersive x-ray (EDX) detector. For particulate density analysis, we analyzed SEM images with the openly available ImageJ software. Plan-view TEM-EDX was performed with a Themis Z S/TEM and JEOL 2010 TEM. For high-resolution analysis, we prepared cross-sectional specimen with a focused ion beam (FIB) (FEI Helios G4 CX) directly from Si_3N_4 TEM grids and imaged them with a double aberration-corrected Thermo Fisher Scientific Themis Z S/TEM, operating at 300 kV. To characterize the structures of the as-deposited and crystallized GaSb thin films, we performed Grazing incidence X-ray diffraction (GIXRD) with a Panalytical Expert Pro X-ray diffractometer using grazing incidence to improve the signal (the angle was chosen to be 0.7°). To characterize the electrical resistivity of the GaSb thin films, we used a van der Pauw (vdP) setup. For stability, Pt/Au with thicknesses of 40 nm/50 nm were deposited as contact electrodes. For the in-situ resistivity measurement, we heated the as-deposited samples with a heating rate of 3 °C/min, continuously registering the resistivity.

3. Results and discussion

3.1. Thin film deposition from powder target

Commercially available targets are the typical starting points for PLD thin film depositions of previously unexplored compositions. Most commercial targets are based on powder sintering and then, for instance, a GaSb target can consist of sintered Ga and Sb powders. Although we start with a target with composition and phase as the desired thin films, composition and transfer yield problems almost always arise due to differences in ablation efficiencies and transfer rates of the individual constituent elements in the target. To overcome these problems and to achieve exact stoichiometric transfer with good yield, relevant process parameters must be optimized: i.e., the laser fluence, the process gas (Ar) partial pressure, and the target-substrate (T-S) distance. For PLD deposition of GaSb thin films we initially started with a single phase stoichiometric $Ga_{50}Sb_{50}$ target obtained commercially from K-TECH. For fast thin film screening with TEM we want to avoid tedious TEM sample preparation. Therefore, we directly deposit thin films on a 20 nm thick amorphous C films on copper grids or sometimes on Si_3N_4 membranes.

Fig. 1 shows TEM Results of GaSb films grown by systematically varying PLD process parameters. The most prominent and interesting result, but not the desired one, is presented in Figures (a)–(c) where the compositions of the films for all possible deposition parameters stay close to $Ga_{40}Sb_{60}$ and thus clearly deviate from the $Ga_{50}Sb_{50}$ target. The deposition yield, i.e. the amount of material transferred onto the substrate depends highly on the deposition parameters. Figures (d)–(f) show the rate of material transfer for different deposition parameters. Here the yields were calculated as follow: for the EDX characterization exactly the same parameters were used. Once the measurements were done, the intensity counts for Ga and Sb were normalized with the intensity count of the amorphous C grid. The results show that increasing laser fluence, decreasing Ar partial pressure, and decreasing T-S distance results in an increase in material transfer from target to substrate. Our results thus show that, although the material transfer is good, it is not

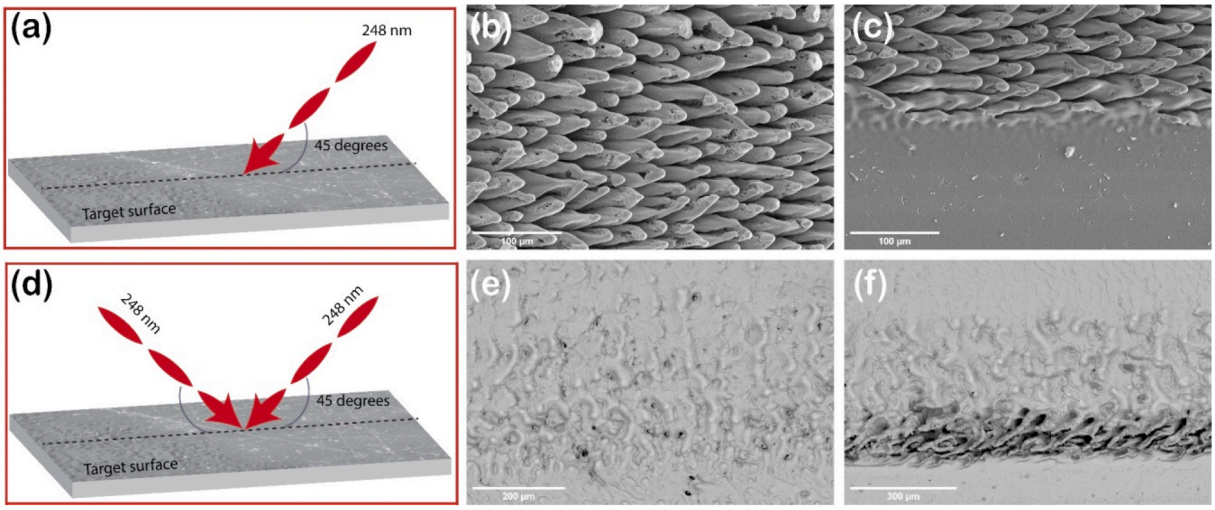

Fig. 3. Schematics of Laser-Target interaction, (a) for a normal PLD deposition scenario and (d) for 180° target rotation. SEM images of the ablated target surfaces show directional pillar formation related to the 45° incidence angle of the laser in (b) and (c). In (e) and (f) pillar formation is suppressed by the 180° rotation.

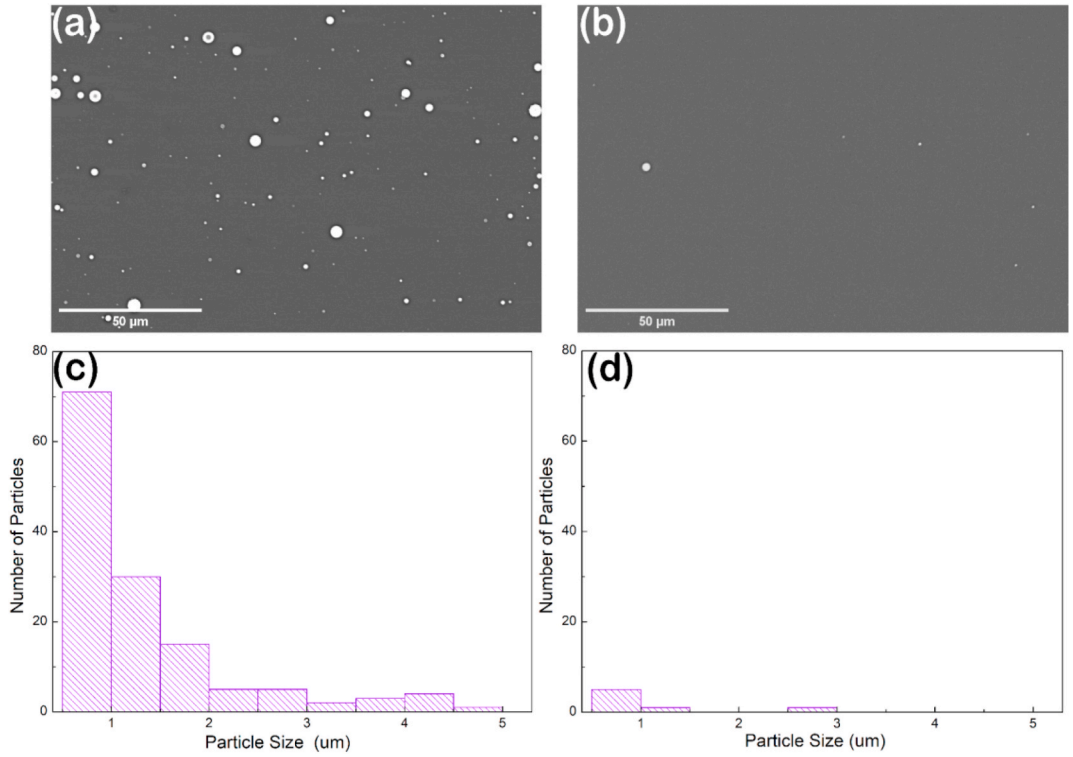

Fig. 4. SEM analysis of particulates, (a) for a normal PLD deposition scenario and (b) for 180° target rotation. The corresponding particulate-size histograms to (a) and (b) are shown in (c) and (d), respectively.

possible to achieve stoichiometric $Ga_{50}Sb_{50}$ thin film using powder sintered GaSb target (within a reasonable PLD parameter range).

3.2. Thin film deposition from polycrystalline target

Depositions from powder sintered GaSb targets, with all possible PLD parameter variations, as shown by Fig. 1 did lead to off-stoichiometric material transfer. However, another major problem that is encountered here, but also reported in the literature, is the presence of high number density Ga-rich particulates on the film surface (see the black spots in Fig. S2 of the SI). In general, the presence of particulates is detrimental, especially to produce devices. Generation of particulates during the laser – target interaction depends on multiple factors which in the end determine the energy density on the target surface [35]. When a high energy laser interacts with a less dense target, the laser pulse penetration depth is large [27]. This causes thermal shock and subsurface superheating due to high energy density on the target surface, leading to particulate generation. One way of reducing the energy density is to increase the density of the target material. Since powder sintered targets are porous, we prepared another target by melting constituent element of Ga and Sb in a vacuum quartz ampule and then cooling the non-porous single phase GaSb back to room temperature.

After polishing the dense target, new PLD depositions were performed, and the Results are shown in Fig. 2. Here the laser fluence and

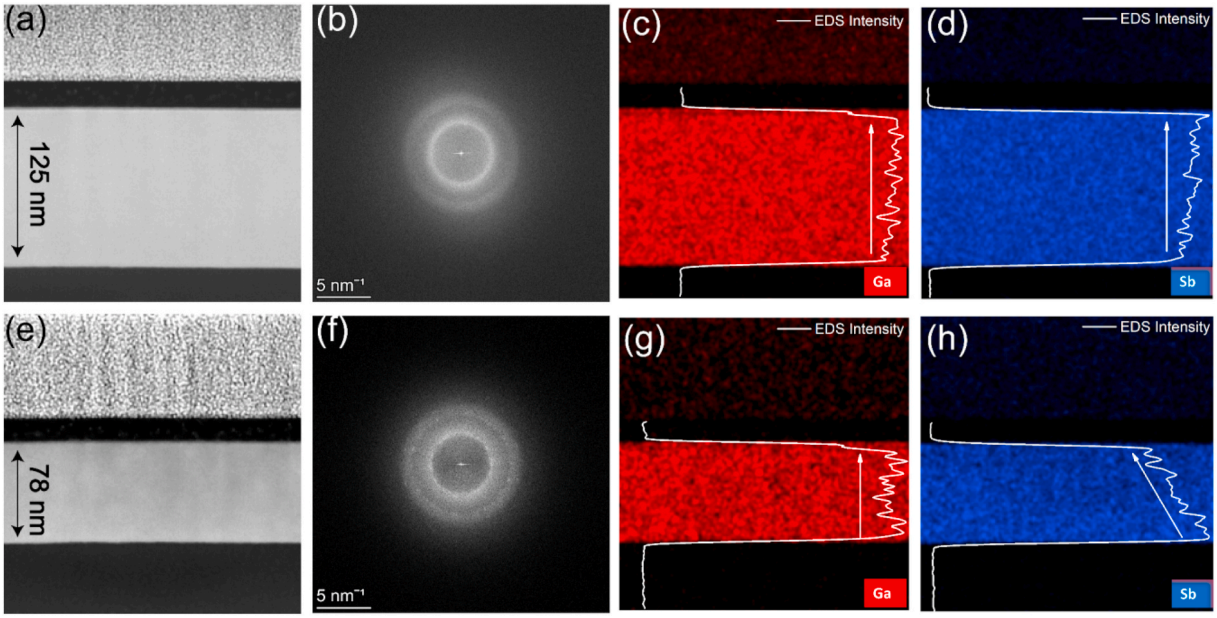

Fig. 5. High-angle annular dark field (HAADF)-STEM images and STEM-EDS chemical composition scan of as-deposited GaSb thin film cross-sections with target rotation (a)–(d) and without target rotation (e)–(h). For films made with a rotation target holder, we see a homogenous chemical composition across the film for both (c) Ga and (d) Sb. Although (g) Ga composition is homogeneous, (h) Sb composition varies linearly across the film for a thin film grown without target rotation.

the T-S distance were fixed at 1.5 J cm^{-2} and 55 mm, respectively. The main objective to reduce the number of particulates is indeed achieved (see Fig. S3 in the SI), although it is still not completely removed. In addition, a film composition very close to the stoichiometric 50:50 can now be obtained (Fig. 2 (a)). However, as seen from the C normalized EDX counts of Ga and Sb (Fig. 2 (b)), the growth rate turns out to be problematically low for high Ar partial pressure depositions. In order to achieve sufficient growth rate low Ar partial pressures (typically 10^{-3} mbar) are required and then the film composition is $Ga_{45}Sb_{55}$, which nevertheless is better than the $Ga_{40}Sb_{60}$ obtained with the commercial target.

Target analysis after laser ablation provides insights in the morphological change on the target surface after laser-target interactions. Fig. 3 (b) and 3 (c) show SEM images of the homemade PLD target at the ablated areas and at the edge between ablated and non-ablated areas, respectively. In Fig. 3 (b) we see that directional pillars are present, whose direction is related to the 45° incident angle of the high-power laser on the target surface after ablating with 5000 laser pulses as schematically presented in Fig. 3 (a). The ablation took place at a fluence of 1.5 J cm^{-2}. Pillar formation during ablation is not desirable for a number of reasons. One problem with the micron-size directional pillars is the spread of the beam energy which then reduce the material transfer by reducing the laser fluence. Another problem with pillar formation is the deviation of plume direction by small angle, towards the laser beam, from the original direction which is normal to the substrate surface [27].

Formation of pillars on the target surface is directly related to a high particulate density on the surface of thin films. Fig. 4 (a) shows an SEM image of a thin film deposited using a dense crystalline GaSb target. Micron-size pillars, as shown in Fig. 3 (b)and 3 (c), lead to a high particulate density in the deposited thin film. The transfer of material from the target to the substrate not only produced a GaSb thin film but also undesired particulates with sizes ranging from sub-100nm to μm as shown in Fig. 4 (c). This problem is known in the PLD literature. We tried a possible solution to reduce pillar formation and to diminish particulates in the thin films: i.e., rotate the PLD target after a limited number of laser pulses with the idea to suppress pillar formation [27,33].

To perform a 180° target rotation and to suppress pillar formation, we designed and implemented a homemade target rotator during thin film depositions (see SI). Fig. 3 (e) and 3 (f) indeed prove that a rotation of 180° after each 1000 laser pulses during PLD, illustrated by Fig. 3 (d), suppresses the pillar formation. Only at the edge between the ablated and non-ablated areas, shown in Fig. 3 (f), pillars still form. This is because it is practically difficult or impossible to perfectly align the two 180° rotated areas on top of each other. Due to the non-perfect overlap of the two rotated areas pillar formation cannot be suppressed in a thin edge region of the ablated area. Although it is interesting that pillar formation at the target surface can be almost completely suppressed, it is of course more relevant what the effect is on the thin film deposition. Fig. 4 (b) and 4 (d) show that the effect is dramatic: we observe a huge reduction in particulates for the films grown using a total number of pulses of 5000. Still, we detect a few particulates for the film shown Fig. 4 (b) and it is very likely that these particulates originate from the edge of the ablated area on the target where the areas after 180° rotation do not perfectly overlap and still some pillar formation occurs.

3.3. STEM-EDX analysis

Plan-view TEM-EDX analyses of the depositions are shown in Fig. S4 (SI), where Fig. S4 (a) is an EDX spectrum of a deposition before and Fig. S4 (b) is after implementation of 180° target rotation. From this analysis it is clear how the dramatic reduction in particulate density, from a 180° target rotation during deposition, in turn leads to production of GaSb thin films with exact stoichiometric composition of $Ga_{50}Sb_{50}$. The main explanation is that the Ga constituent increased in the film due to the reduction of Ga-rich particulates. This leads to an atomic percentage increase in elemental Ga from Ga_{45} to Ga_{50}. To better understand the film composition across their thicknesses, we prepared cross-section TEM samples for both films shown in Fig. 4. Fig. 5 shows the HAADF-STEM images and STEM-EDX analyses for two samples, with and without 180° target rotation.

Fig. 5 (a)–(d) show Results for the sample with target rotation, while Fig. 5 (e)–(h) show the results for the sample without target rotation. Here three basic differences between the two samples can be observed. The first and the most obvious observation is the thickness difference between the two samples for the same deposition parameters shown in Fig. 5 (a) and (e). By introducing 180° target rotation we noticed a 60% increase in thickness. The second difference is in the Fast Fourier

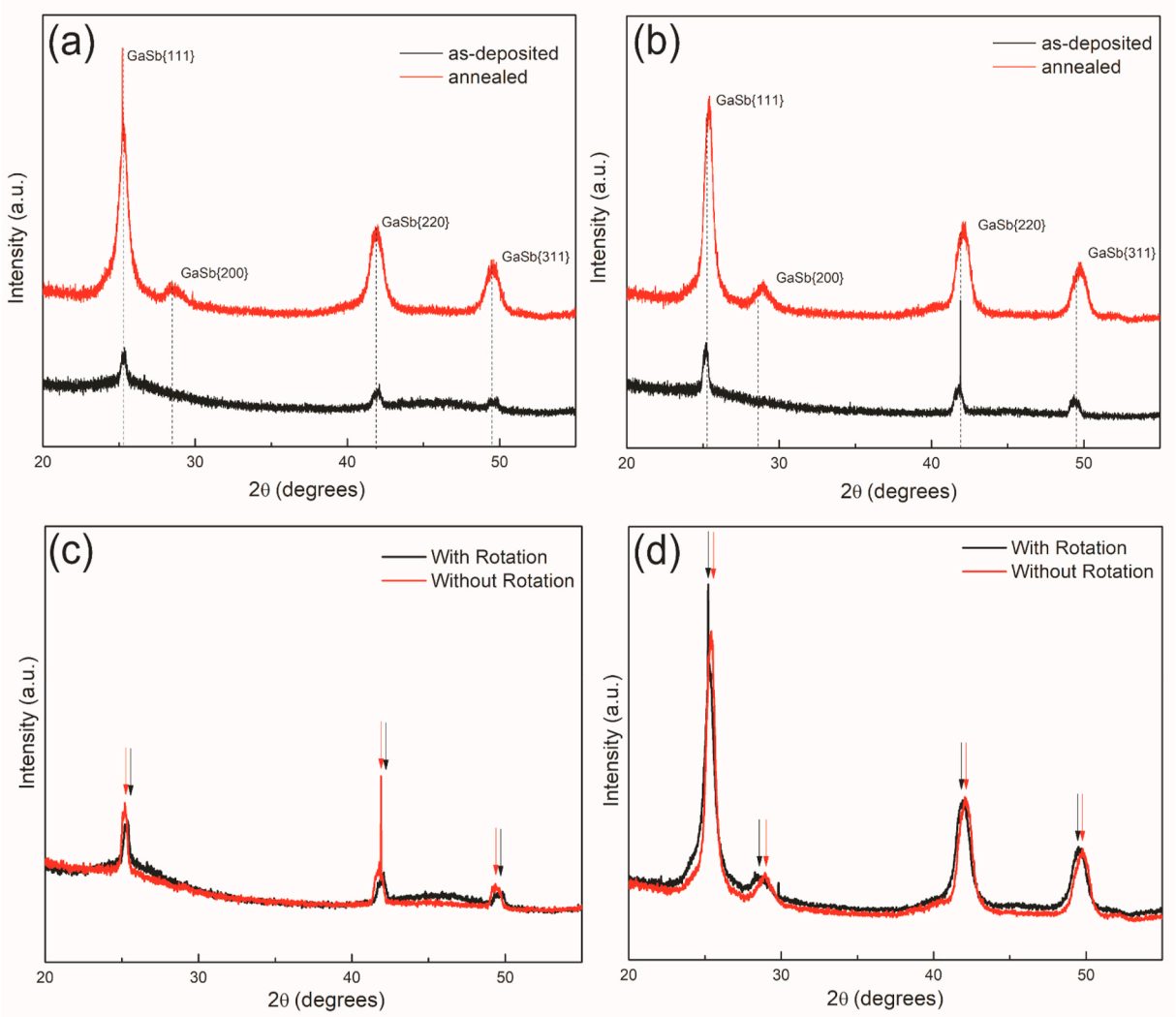

Fig. 6. XRD spectra for the as-deposited and annealed samples prepared (a) with and (b) without a 180° target rotation. Comparing intensities of the as deposited samples (c), we see that the sample without rotation shows more pronounced peaks. (d) XRD intensity comparison of annealed samples with and without rotation. A shift in peak positions is observed for both as-deposited and annealed samples.

Transform (FFT) images, Fig. 5 (b) and (f), extracted from the HAADF images. In Fig. 5 (f) intense diffraction spots are visible initially in the as-deposited phase for the sample made without rotation. This indicates the presence of small crystallites embedded in the amorphous matrix. Finally, from the STEM – EDX mapping, a homogeneous elemental distribution across the film thickness is visible for the sample made with 180° target rotation in Fig. 5 (c) and (d). Fig. 5 (h) shows that the Sb elemental composition changes linearly across the film thickness for the sample made without target rotation. This Sb composition variation during growth, and thus during (increasing) pillar formation, is a direct explanation for the composition shifting away from the stochiometric $Ga_{50}Sb_{50}$.

The presence of crystallites in the amorphous matrix can be explained by the laser – target interaction and the process gas pressure in the PLD chamber. The high energy laser interaction with the target surface is powerful enough to eject not only macroscopic particulates but also microscopic crystallites. It is especially easy when directional pillars form since the pillars tip can easily break during ablation producing crystallites in the amorphous matrix in addition to the particulates. This will undermine the quality of the deposited thin films. Another reason for crystallite formation is due to the process gas pressure during ablation. At low gas pressure, the ablated materials from the laser-target interaction will acquire enough kinetic energy. When reaching the substrate, the ablated materials would have high surface mobility, which usually would have been triggered by external thermal energy, to produce crystallites [36]. In addition, at high process gas pressure the ablated materials can condensate in the gas phase to form small size crystallites before reaching the substrate [37]. In general, since their formation is due to multiple reasons, a complete removal of crystallites in the amorphous matrix is an exceedingly difficult task in PLD. Indeed, suppressing the pillar formation of the target surface was expected to increase the material transfer since pillar formation directly affect the material transfer by reducing the laser fluence and by shifting the plume away from the substrate surface [27]. However, one would assume that, increasing material transfer with target rotation, would also means an increasing crystallite density in the as-deposited phase. Interestingly, we observe the opposite effect. From our Results, although not completely free, nearly crystallite free thin films with a smooth surface can be produced by employing a 180° target rotation.

3.4. GIXRD analysis

For an insight into the structural properties of the films, we performed GIXRD measurements for both samples shown in Fig. 4 (a) and (b). The measurements were recorded before and after annealing the samples at 300 °C. Fig. 6 (a) and (b) show the appearance of small peaks

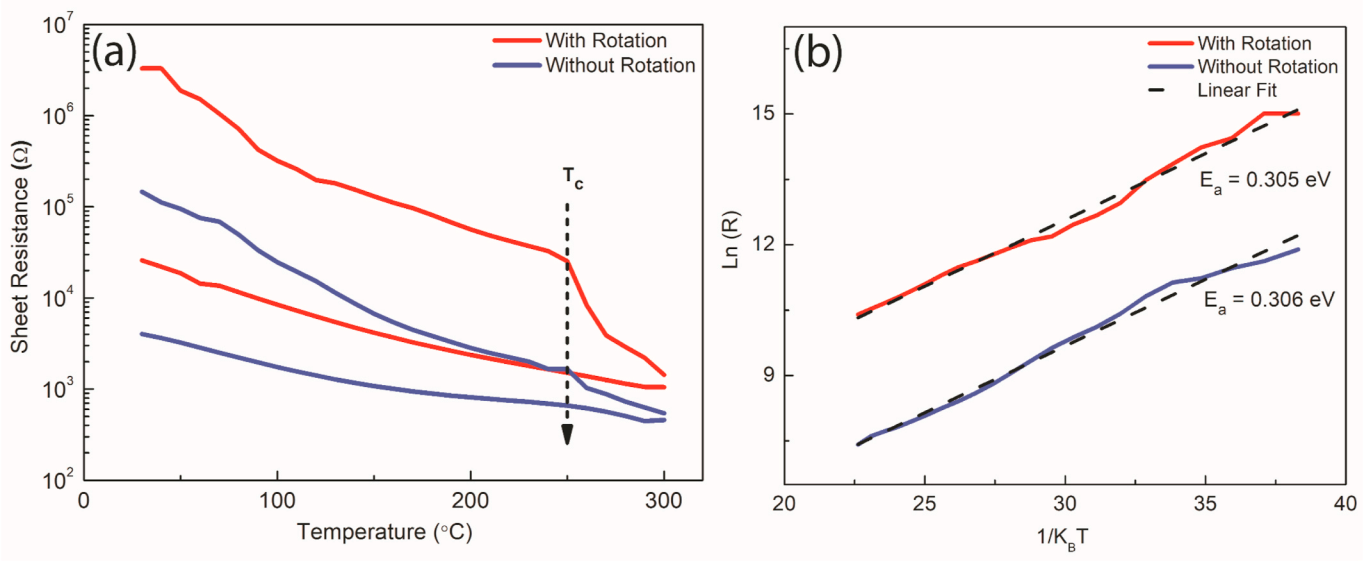

Fig. 7. Van der Pauw resistivity vs. temperature measurements for the as-deposited samples prepared with and without a 180° target rotation are presented in (a), with their activation energy fitted lines given in (b). For both samples, the crystallization temperature is 250 °C.

already in the as-deposited phases for both samples. This indicates that the GaSb films are partially crystalline even when the PLD process is performed (with the substrate) at room temperature. Comparing intensities of the as deposited samples, in Fig. 6 (c), shows that the sample without rotation has more pronounced peaks. This indicates the presence of a higher number of crystallites in the amorphous matrix for the sample without target rotation. Going back to the FFTs in Fig. 5 (b) and (f), this is exactly what is visible there as well. After the annealing, intense diffraction peaks at 2θ = 25.28°, 28.47°, 41.9°, and 49.54° appear for both samples corresponding to the {111}, {200}, {220}, and {311} planes of cubic GaSb. The produced GaSb phase has a space group of Fm-3m with a lattice parameter of 6.09 Å corresponding to the Zinc Blende structure.

Fig. 6 (c) and (d) show the XRD intensity comparison for samples prepared with and without 180° target rotation for both as-deposited and annealed phases respectively. Looking closely, we notice a shift in peak positions for both cases. Slight peak shifts towards smaller 2θ values are recorded for the as-deposited film without rotation. More Sb is present according to the EDX for the film without rotation (Fig. S4 in SI). Since the atomic radius of Sb is slightly bigger than that of Ga, a sample with more Sb thus has a slightly larger lattice parameter, in agreement with the observation for the as-deposited films. However, after annealing, the peak shift for the sample without rotation is opposite to what was observed in the as-deposited case. The peak shifts towards larger 2θ values indicate a decreasing lattice parameter. This is potentially due to intermixing of the Ga-rich particulates on the film surface with the film upon annealing leading to an increasing Ga concentration in the sample observed by XRD. Compared to samples with 180° target rotation, non-rotated samples suffer from phase separation and lattice parameter changes upon annealing. For PCM application, this is not ideal. The GaSb thin films produced with 180° target rotation have a strong structural integrity in both the as-deposited and annealed phases. This fact makes the material highly suited for PCM devices.

3.5. Electrical characterizations

Electrical resistance vs. temperature measurements are shown in Fig. 7 (a) for two samples: one produced with target rotation, and one without. We used a heating rate of 3 °C/min. For both as-deposited samples, the resistivity continuously decreases with increasing temperature. This continuous decrease is met with a sudden drop in measured resistivity value exactly at the crystallization temperature Tx: i.e., where the amorphous to crystalline phase transformation occurs. For both samples, the phase transformation happened at 250 °C. The observed Tx temperature for our films is higher when compared with previous reported values [17,38]. Note the resistivity contrast between the amorphous and the crystalline phases for both samples in Fig. 7 (a). The sample without target rotation has a lower resistivity value for both the as-deposited and the crystalline phases. One reason for this might be the high-density of Ga-rich particulates on the thin film surface that contributes to an increase in conductivity. Another more prominent reason is the fact that the film is off-stoichiometric with excess Sb. Previous works on multiple alloys of GaSb showed a clear reduction of resistivity with increasing Sb content [17,19]. The activation energies for conduction in the as-deposited 'amorphous' phase was extracted from the linear relationship between Ln(R) and the inverse of the temperature range used in the measurements. Fig. 7 (b) show the fitted values for the activation energy of conduction extracted for both samples are the same.

For application as a PCM device, a distinct contrast in electrical resistivity or optical reflectivity between the amorphous and crystalline phases of the thin film is an important requirement. Several orders of magnitude difference will produce distinct states for the SET and RESET operations. From our electrical characterization only two orders of magnitude contrast is achieved at room temperature for $Ga_{50}Sb_{50}$ thin films. This is relatively low when compared with typical phase change materials like GST or Sb_2Te_3. However, for GaSb the crystalline phase resistivity is highly dependent on the annealing step used and by varying the maximum annealing temperature it was possible to increase the resistivity difference between the phases as high as 5 orders [39]. Moreover, an important drawback of most used PCMs (like GST) is that the SET resistivity is low such that a high RESET current and power is required for switching. The present GaSb films exhibit a substantially larger resistivity showing the promise of lower power operation. This makes the material very suitable for PCM application, but previous studies suffered from phase separation with separate crystallization of the excess Sb in the $Ga_{45}Sb_{55}$ alloy [17]. Our ability to produce a perfect stoichiometric $Ga_{50}Sb_{50}$ film will be a huge benefit in reducing the phase separation and additional Sb crystallization in the PCM device at high annealing temperature.

4. Conclusions

In summary, GaSb films from both powder-sintered and dense molten targets were produced using PLD. We show that, for a wide range of deposition parameters, the deposited films were off-stoichiometric and contained micron-sized particulates. We also show that pillars, which are produced by the directional nature of the laser-target interaction, are directly responsible for the thin film quality and particulate formation. The pillar formation can be simply, but elegantly, suppressed using a 180° target rotation after a limited number of pulses (e.g. 1000 in our case). S/TEM analyses on films deposited using target rotation show a 60% increase in yield, large decrease in particulate density, and exact $Ga_{50}Sb_{50}$ stoichiometric transfer from the target. The measured XRD spectra for a film produced with target rotation show a strong structural integrity in both the as-deposited and annealed phases. For a film deposited without target rotation, in addition to the off-stoichiometric composition and high density of particulates on the surface, the XRD spectra show that the Ga-rich particulates intermix with the film at elevated temperature (300 °C). Sheet resistance measurements of the $Ga_{50}Sb_{50}$ thin films show a high crystallization temperature of 250 °C and a high resistivity of the crystalline phase reducing the resistance contrast between the amorphous and crystalline phases to about two orders of magnitude. We believe the properties of the GaSb films we produced by 180° target rotation are attractive for future optoelectronic and PCM applications.

Author contribution

Daniel T. Yimam: Conceptualization, Methodology, Investigation, Writing – original draft, Visualization Heng Zhang: Investigation, Writing – review & editing Jamo Momand: Investigation, Writing – original draft, Visualization, Supervision Bart J. Kooi: Conceptualization, Writing – review & editing, Supervision, Project administration, Funding acquisition

Declaration of competing interest

The authors declare that they have no known competing financial interests or personal relationships that could have appeared to influence the work reported in this paper.

Acknowledgments

This project has received funding from the European Union's Horizon 2020 Research and Innovation Programme "BeforeHand" (Boosting Performance of Phase Change Devices by Hetero- and Nanostructure Material Design)" under Grant Agreement No. 824957.

Appendix A. Supplementary data

Supplementary data to this article can be found online at https://doi.org/10.1016/j.mssp.2021.105965.

References

[1] S. Lai, Current status of the phase change memory and its future, in: Tech. Dig. - Int. Electron Devices Meet, 2003, pp. 255–258, https://doi.org/10.1109/iedm.2003.1269271.
[2] G.W. Burr, M.J. BrightSky, A. Sebastian, H.Y. Cheng, J.Y. Wu, S. Kim, N.E. Sosa, N. Papandreou, H.L. Lung, H. Pozidis, E. Eleftheriou, C.H. Lam, Recent progress in phase change memory technology, IEEE J. Emerg. Sel. Top. Circuits Syst. 6 (2016) 146–162, https://doi.org/10.1109/JETCAS.2016.2547718.
[3] H.-S.P. Wong, S. Raoux, S. Kim, J. Liang, J.P. Reifenberg, B. Rajendran, M. Asheghi, K.E. Goodson, Phase change memory, Proc. IEEE 98 (2010) 2201–2227, https://doi.org/10.1109/JPROC.2010.2070050.
[4] M. Wuttig, N. Yamada, Phase-change materials for rewriteable data storage, Nat. Mater. 6 (2007) 824–832, https://doi.org/10.1038/nmat2009.
[5] M.R. King, N. El-Hinnawy, M. Salmon, J. Gu, B.P. Wagner, E.B. Jones, P. Borodulin, R.S. Howell, D.T. Nichols, R.M. Young, Morphological analysis of GeTe in inline phase change switches, J. Appl. Phys. 118 (2015), 094501, https://doi.org/10.1063/1.4929419.
[6] A. Pirovano, An introduction on phase-change memories, Phase Chang. Mem. Device Physics, Reliab. Appl. (2017) 1–10, https://doi.org/10.1007/978-3-319-69053-7_1.
[7] N. Yamada, E. Ohno, K. Nishiuchi, N. Akahira, M. Takao, Rapid-phase transitions of GeTe-Sb2Te3 pseudobinary amorphous thin films for an optical disk memory, J. Appl. Phys. 69 (1991) 2849–2856, https://doi.org/10.1063/1.348620.
[8] A. Pirovano, A.L. Lacaita, F. Pellizzer, S.A. Kostylev, A. Benvenuti, R. Bez, Low-field amorphous state resistance and threshold voltage drift in chalcogenide materials, IEEE Trans. Electron. Dev. 51 (2004) 714–719, https://doi.org/10.1109/TED.2004.825805.
[9] D. Ielmini, S. Lavizzari, D. Sharma, A.L. Lacaita, Physical interpretation, modeling and impact on phase change memory (PCM) reliability of resistance drift due to chalcogenide structural relaxation, in: Tech. Dig. - Int. Electron Devices Meet, IEDM, 2007, pp. 939–942, https://doi.org/10.1109/IEDM.2007.4419107.
[10] A. Sebastian, D. Krebs, M. Le Gallo, H. Pozidis, E. Eleftheriou, A collective relaxation model for resistance drift in phase change memory cells, in: IEEE Int. Reliab. Phys. Symp. Proc., Institute of Electrical and Electronics Engineers Inc., 2015, pp. MY51–MY56, https://doi.org/10.1109/IRPS.2015.7112808.
[11] K. Kim, S.J. Ahn, Reliability investigations for manufacturable high density PRAM, IEEE Int. Reliab. Phys. Symp. Proc. (2005) 157–162, https://doi.org/10.1109/relphy.2005.1493077.
[12] Z. Sun, J. Zhou, A. Blomqvist, B. Johansson, R. Ahuja, Formation of large voids in the amorphous phase-change memory Ge2Sb2Te5 alloy, Phys. Rev. Lett. 102 (2009), 075504, https://doi.org/10.1103/PhysRevLett.102.075504.
[13] T.Y. Yang, J.Y. Cho, Y.J. Park, Y.C. Joo, Influence of dopants on atomic migration and void formation in molten Ge 2Sb 2Te 5 under high-amplitude electrical pulse, Acta Mater. 60 (2012) 2021–2030, https://doi.org/10.1016/j.actamat.2011.12.034.
[14] P. Zuliani, E. Palumbo, M. Borghi, G. Dalla Libera, R. Annunziata, Engineering of chalcogenide materials for embedded applications of Phase Change Memory, Solid State Electron. 111 (2015) 27–31, https://doi.org/10.1016/j.sse.2015.04.009.
[15] K.-J. Choi, S.-M. Yoon, N.-Y. Lee, S.-Y. Lee, Y.-S. Park, B.-G. Yu, S.-O. Ryu, The Effect of Antimony-Doping on Ge2Sb2Te5, a Phase Change Material, 2008, https://doi.org/10.1016/j.tsf.2008.02.014.
[16] S. Privitera, E. Rimini, C. Bongiorno, A. Pirovano, R. Bez, Effects of dopants on the amorphous-to-fcc transition in Ge2Sb2Te5 thin films, Nucl. Instrum. Methods Phys. Res. Sect. B Beam Interact. Mater. Atoms 257 (2007) 352–354, https://doi.org/10.1016/j.nimb.2007.01.265.
[17] M. Putero, M.V. Coulet, T. Ouled-Khachroum, C. Muller, C. Baehtz, S. Raoux, Unusual crystallization behavior in Ga-Sb phase change alloys, Apl. Mater. 1 (2013), https://doi.org/10.1063/1.4833035.
[18] S. Raoux, A.K. König, H.Y. Cheng, D. Garbin, R.W. Cheek, J.L. Jordan-Sweet, M. Wuttig, Phase transitions in Ga-Sb phase change alloys, Phys. Status Solidi Basic Res. 249 (2012) 1999–2004, https://doi.org/10.1002/pssb.201200370.
[19] Y. Lu, S. Song, Z. Song, B. Liu, Ga14Sb86 film for ultralong data retention phase-change memory, J. Appl. Phys. 109 (2011), https://doi.org/10.1063/1.3563067.
[20] Q. Yin, L. Chen, Crystallization behavior and electrical characteristics of Ga–Sb thin films for phase change memory, Nanotechnology 31 (2020) 215709, https://doi.org/10.1088/1361-6528/AB7429.
[21] M. Putero, M.V. Coulet, C. Muller, G. Cohen, M. Hopstaken, C. Baehtz, S. Raoux, Density change upon crystallization of Ga-Sb films, Appl. Phys. Lett. 105 (2014), https://doi.org/10.1063/1.4901321.
[22] P.A. Vermeulen, D.T. Yimam, M.A. Loi, B.J. Kooi, Multilevel reflectance switching of ultrathin phase-change films, J. Appl. Phys. 125 (2019) 193105, https://doi.org/10.1063/1.5085715.
[23] M. Bouška, S. Pechev, Q. Simon, R. Boidin, V. Nazabal, J. Gutwirth, E. Baudet, P. Němec, Pulsed laser deposited GeTe-rich GeTe-Sb2Te3 thin films, Sci. Rep. 6 (2016) 1–10, https://doi.org/10.1038/srep26552.
[24] A. Lotnyk, I. Hilmi, U. Ross, B. Rauschenbach, Van der Waals interfacial bonding and intermixing in GeTe-Sb2Te3-based superlattices, Nano Res 11 (2018) 1676–1686, https://doi.org/10.1007/s12274-017-1785-y.
[25] A. Lotnyk, I. Hilmi, M. Behrens, B. Rauschenbach, Temperature dependent evolution of local structure in chalcogenide-based superlattices, Appl. Surf. Sci. 536 (2021) 147959, https://doi.org/10.1016/j.apsusc.2020.147959.
[26] J. Feng, A. Lotnyk, H. Bryja, X. Wang, M. Xu, Q. Lin, X. Cheng, M. Xu, H. Tong, X. Miao, "stickier"-Surface Sb2Te3Templates enable fast memory switching of phase change material GeSb2Te4with growth-dominated crystallization, ACS Appl. Mater. Interfaces 12 (2020) 33397–33407, https://doi.org/10.1021/acsami.0c07973.
[27] D.P. Norton, Pulsed laser deposition of complex materials: progress toward applications. Pulsed Laser Depos. Thin Film, John Wiley & Sons, Inc., Hoboken, NJ, USA, 2006, pp. 1–31, https://doi.org/10.1002/9780470052129.ch1.
[28] S.J. Barrington, R.W. Eason, Effect of Particulate Density on Performance of Waveguide Lasers Grown by Pulsed Laser Deposition, 2000, https://doi.org/10.1109/cleo.2000.907058.
[29] P.K. Schenck, M.D. Vaudin, D.W. Bonnell, J.W. Hastie, A.J. Paul, Particulate reduction in the pulsed laser deposition of barium titanate thin films, Appl. Surf. Sci. 127–129 (1998) 655–661, https://doi.org/10.1016/S0169-4332(97)00721-6.
[30] E. György, I.N. Mihailescu, M. Kompitsas, A. Giannoudakos, Deposition of particulate-free thin films by two synchronised laser sources: effects of ambient gas pressure and laser fluence, Thin Solid Films 446 (2004) 178–183, https://doi.org/10.1016/j.tsf.2003.09.071.

[31] T. Yoshitake, G. Shiraishi, K. Nagayama, Elimination of droplets using a vane velocity filter for pulsed laser ablation of FeSi 2, in: Appl. Surf. Sci, Elsevier, 2002, pp. 379–383, https://doi.org/10.1016/S0169-4332(02)00344-6.
[32] E. Agostinelli, S. Kaciulis, M. Vittori-Antisari, Great reduction of participates in pulsed laser deposition of Ag-Co films by using a shaded off-axis geometry, Appl. Surf. Sci. 156 (2000) 143–148, https://doi.org/10.1016/S0169-4332(99)00490-0.
[33] J.J. Prentice, J.A. Grant-Jacob, S.V. Kurilchik, J.I. Mackenzie, R.W. Eason, Particulate reduction in PLD-grown crystalline films via bi-directional target irradiation, Appl. Phys. A 125 (2019) 152, https://doi.org/10.1007/s00339-019-2456-5.
[34] F. Sava, C.N. Borca, A.C. Galca, G. Socol, D. Grolimund, C. Mihai, A. Velea, Structural characterisation and thermal stability of SnSe\GaSb stacked films, Philos. Mag. A 99 (2019) 55–72, https://doi.org/10.1080/14786435.2018.1529442.
[35] N. 1973- Popovici, Oxide Thin Films for Spintronics Application Growth and Characterization, 2009. https://repositorio.ul.pt/handle/10451/1635. accessed March 7, 2021.
[36] T. García, E. De Posada, R. Diamant, J.L. Peña, Textured thin films grown at room temperature by laser ablation, in: Appl. Phys. A Mater. Sci. Process., Springer Verlag, 2004, pp. 919–921, https://doi.org/10.1007/s00339-004-2851-3.
[37] T. Sasaki, S. Terauchi, N. Koshizaki, H. Umehara, The preparation of iron complex oxide nanoparticles by pulsed-laser ablation, Appl. Surf. Sci. 127–129 (1998) 398–402, https://doi.org/10.1016/S0169-4332(97)00663-6.
[38] A. Velea, C.N. Borca, G. Socol, A.C. Galca, D. Grolimund, M. Popescu, J.A. van Bokhoven, *In-situ* crystallization of GeTe\GaSb phase change memory stacked films, J. Appl. Phys. 116 (2014) 234306, https://doi.org/10.1063/1.4904741.
[39] H.-Y. Cheng, S. Raoux, K.V. Nguyen, R.S. Shenoy, M. BrightSky, Ga 46 Sb 54 material for fast switching and Pb-free soldering reflow process complying phase-change memory, ECS J. Solid State Sci. Technol. 3 (2014) P263–P267, https://doi.org/10.1149/2.011407jss.